Synthesizing a novel Fe/Al/Zr-incorporated cross-linked chitosan as absorbent for effective removal of fluoride from aqueous solution

Abstract: Fe/Al/Zr modified chitosan beads was synthesized in this study as a potential adsorbent to adsorb fluoride from water. Series of adsorption experiments were carried out to test the fluoride removal performance of the new adsorbent and probe its adsorption mechanism. It was found that an adsorption capacity of 36.04 mg fluoride /g Chitosan beads was achieved in the conditions with pH at 6.0, 1.6 g/L of the dosage of CS-ZFA, 60 mg/L of initial concentration of fluoride, and 120 min adsorption time. The adsorption kinetics followed a pseudo-second-order model, and the adsorption isotherm can be described by the Freundlich isotherm model. Furthermore, various characterization methods were adopted to characterize the prepared adsorbent. Based on the characterization, the high adsorption capacity of the newly synthesized adsorbent is due to the electrostatic attraction and the formation of CS-ZFA-F complex.

Keywords: fluoride; chitosan; modification, adsorption; electrostatic attraction,

1. Introduction

Fluoride, one of the important microelements in human bodies, is closely related to human life activities and skeletal tissue metabolism. It is also the umbrella of teeth to prevent tooth decay. . However, our demand for fluoride is limited. Long-term intake of high concentration of fluoride can result in excess fluoride accumulation in bodies. The accumulated fluride can react with Ca^{2+} in the bones, reducing the absorption of calcium, and thus eventually leading to systemic diseases such as

damage of teeth, bone and the cardiovascular and nervous systems [1]. The permissible limit of fluoride recommended by World Health Organization (WHO) is 1.5 mg/L [2], while Chinese government has set a harsher guidance value as1.0 mg/L for fluoride in ?? drinking water according to Chinese Standard [3]. Fluoride pollution is common in industrial wastewater from aluminum and steel production, metal surface treatment, and semiconductor manufacturing [4]. Therefore, it is very necessary to take effective measures to reduce the concentration of fluoride in water.

So far, extensive research has been carried out to remove fluoride from water, which includes precipitation-coagulation [5, 6], ion exchange [7, 8], membrane technology [9, 10], dialysis [11, 12] and adsorption processes [13-16]. In last decades, adsorption technique is widely used to remove fluoride from water due to the easy availability of raw materials to make adsorbents, low energy requirement, ease of design and the possibility of reusing the adsorbent via regeneration. Various kinds of materials such as natural minerals [17, 18], metal oxides [19, 20], biomass [21, 23], hydrotalcites [24, 25], ion exchange resins [26], have been used as adsorbents. However, a common problem for adsorption is that adsorbents have insufficient sorption capacity. In addition, powdered adsorbents are not conducive to be recovered after adsorption for reuse. These problems greatly impede the real application of adsorption. Therefore, there is urgent need to develop efficient adsorbents to overcome the problems identified above for contaminant removal from water.

Among various materials as adsorbents, chitosan (CS) as a natural material has drawn a significant attention for real application due to its abundance, antibacterial,

high affinity toward dyes and metals, biodegradability and good biocompatibility. In recent years, using CS and its blends as adsorbents has been extensively investigated for the removal of metals [27-29], but its application for fluoride adsorption is rare. CS has high solubility in acid, thus, it cannot be directly used as an adsorbent for ???. Enhancement of acid resistance is needed, for example, through crosslinking (add reference). . However, crosslinking may decrease the adsorption capacity of CS because of the decrease in free amino groups which is [30]. So we need to modify the chitosan to improve its adsorption capacity and selectivity. (this whole paragraph is not very clear and specific. You could revise this paragraph by rewriting 1) acid resistance 2) adsorption capacity 3) selectivity. But it would be better to use specific references and data to demonstrate these three are real challenges that we need to address)

In recent years, a metal composite adsorbent prepared by a one-step co-precipitation method was developed for the treatment of fluorine-containing wastewater. (explain here why metal composite is good (reason)) For example, Wang Mei et al. [31] synthesized the Mg-Al-Zr metal composite using a one-step co-precipitation method, which obtained a fluoride adsorption capacity of 22.9 mg/g, ??? higher than the control with??. Yang Yu et al. [32] synthesized a Fe-Mg-La metal complex by one-step co-precipitation method, and the fluoride adsorption capacity reached as high as 270.3 mg/g at pH 4.0. Moreover, this adsorbent demonstrated a high selectivity. The co-existence of anions such as Cl^- and CO_3^{2-} in the aqueous solution hardly interfered with the fluoride adsorption. The

characterization of adsorbents by FTIR, XPS and other methods showed that the adsorption of F^- was achieved mainly by ion exchange. Although the metal composite adsorbent synthesized by the co-precipitation method has a large adsorption capacity for F^-, its disadvantage is that the synthesized substance is in powder form, which is not conducive to separation from the liquid. (this paragraph is relatively weak. You only cited two papers and both of them are from china. Could you review more? For example, add what metals should be used etc)

metals on absorbents can generate $M(OH)_n$ through hydrolysison absorbent surface in aqueous solution. Anions in the water can exchange with hydroxidein some conditions and thus be adsorbed to absorbentson for anions removal [33]. Ligand exchange with anions is dependent on metal types, thus, carefully selecting metal types could improve the anion selectivity of absorbents. In addition, $-NH_2$ and -OH on chitosan have a strong coordination effect on metal ions, and the formation of coordination bonds can make the product positively charged, thus enhancing the adsorption capacity of chitosan to anions in water [34]. Based on this mechanism, it is expected that , using metals to modify chitosan could improve the adsorption capacity and selectivity of chitosan microspheres to F^-.

This paper thus aimed to use ferric nitrate, zirconium nitrate and aluminum sulfate to modify natural polymer chitosan with the co-precipitation method to synthesize metal modified chitosan microspheres (CS-ZFA) as absorbents for fluoride removal from aqueous solutions. Furthermore, effects of pH and coexistence of ions on fluoride adsorption, adsorption kinetics, adsorption isotherm, were studied to

investigate fluoride adsorption performance and mechanism of the newly synthesized chitosan absorbents. Finally, the regeneration of CS-ZFA was investigated to explore its reusability.

2. Materials and Methods

2.1. Chemicals and aaterials

The stock solution of F^- (100 mg/L) was prepared by dissolving NaF into distilled water. F^- solutions with different concentrations were freshly prepared by diluting the stock solution with distilled water. The chemicals such as $Al_2(SO_4)_3 \cdot 18H_2O$, $Fe(NO_3)_3 \cdot 9H_2O$, $Zr(NO_3)_4 \cdot 5H_2O$, NaF, NaOH, $(C_6H_{11}NO_4)_n$, C_3H_5ClO used in the study were purchased from Kelong chemical reagent factory (Chengdu, China). All chemicals and reagents used in experiments are of analytical grade. Chitosan was (supplement acetic acid)

2.2. Preparation of adsorbent

A chitosan solution was prepared by dissolving chitosan (1 g) into 50 mL 2% acetic acid solution. ?? ml chitosan solution was added to ?? ml 0.37M NaOH solution by using a 1 mL syringe (with needle or not?) in a dropwise manner to form chitosan beads, which werewashed with deionized water until the pH reaches neutral. The washed chitosan beads were soaked into 2.5% epichlorohydrin solution for 23 h for ???? (explain for what.) [35, 36]. After this, the beads were washed with deionized water twice.

Different amounts of /Zr/Fe/Al mixed solutions were y for the impregnation of

chitosan beads for 12 h. Then, the CS-ZFA beads were washed with deionized water to remove excess metal solution. The metal modified beads were cured in 2.5% epichlorohydrin solution for 5 h. The composite was retrieved, washed with deionized water several times and dried at 40 ℃ for 24 h. The dried beads were denoted as CS-ZFA. Unmodified chitosan beads were prepared as controls by the same method but without impregnation in the ZFA solutions

2.3. Material characterization of absorbents

FTIR of CS-ZFA and CS-ZFA-F were measured by a spectrometer (WQF520, China). The surface morphology of samples was observed by using a scanning electron microscopy (SEM, JSM-7500F). EDS and EMI of CS-ZFA absorbents after fluoride adsorption were obtained by Transmission Electron Microscopy-Energy Dispersive X-ray Spectroscope (EDXS, Genesis XM2 system, USA EDAX Corp). The changes in physical and chemical properties of CS and CS-ZFA with temperature were monitored by using the thermal gravity analysis (TGA, NETZSCH STA 449F3) under air atmosphere scanned from 28 to 1000 ℃.

2.4. Adsorption experiments

The pHs of the 100 mg/L fluoride solutions were adjusted with 0.1M NaOH or 0.1M HCl solution. 0.08 g absorbents were added into fluoride solutions held in conical flasks for all adsorption experiments except the study on the adsorption dose.

The adsorption isotherm experiments were studied with different initial fluoride concentrations ranging from 10 to 100 mg/L. The adsorption experiment was conducted for 360 min to figure out the time taken to reach adsorption equilibrium. All adsorption experiments were carried out in a shaking table at 180 rpm and 25 ± 1 ℃.

The initial fluoride concentration and solution pH were 60 mg/L and 6.0 unless otherwise stated.

The concentration of fluoride in the solution was measured by fluoride ion electrode. The adsorption capacity (q_e mg/g) was calculated according to the equation below [37]:

$$q_e = \frac{(C_0 - C_e)V}{m} \quad (1)$$

Where, q_e was the equilibrium adsorption capacity (mg/g); C_0 and C_e were the initial and equilibrium concentration of fluoride in solution; V was the volume of solution and m was the mass of absorbent dosed for adsorption.

3. Results and discussion

3.1. Characterization of adsorbents

Surface morphology of CS-ZFA absorbents before and after fluoride adsorption was shown in Figure 1. It can be seen from Figures 1a and 1b that the surface of the adsorbent before adsorption was relatively rough with abundant protuberances and pores, indicating that the CS-ZFA absorbent was a porous material with high specific surface area. The morphology of the absorbent after adsorption in Figure 1c shows that the surface was smoother than the adsorbent before fluoride adsorption and , and no visible holes can be observed. A new fluorine peak was observed in the EDS spectra after the fluorine adsorption by the absorbent (Figure 2), confirming the F^- adsorption onto CS-ZFA.

FTIR spectra analysis was used to examine the functional groups of the absorbents. The FTIR spectra of CS-ZFA before and after fluoride adsorption is shown in Figure 3. It is found that CS-ZFA had a wide and smooth peak at 3560 cm^{-1}, which was attributed to the stretching vibration of -OH and -NH. The peak of fluoride adsorbed CS-ZFA, however, was red-shifted to 3442 cm^{-1}, indicating that the

amino group not coordinated with metal ions on the chitosan also reacted with the adsorbent [38]. It was found that the stretching vibration peak of -CH in 2920 cm^{-1} after fluoride adsorption was the same as that in the original CS-ZFA of -CH and $-CH_2$, but the peak was weak. The peak at 1625 cm^{-1} corresponds to the stretching vibration of C-O. CS-ZFA had a peak at 1380 cm^{-1}, which was a symmetric bending vibration peak of -CH, and the peak blue shift after adsorption of F^-. The bands around at 1074 cm^{-1} was the peak of Fe-OH, and after the adsorption of F^-, the peak shape was more obvious and there was no stray peak. This indicates that Fe^{3+} played a certain role in the adsorption process. What's more, there was a peak of Al-O at 609 cm^{-1} [39], which changed in all the adsorbed CS-ZFA. The vibration peak of Zr-F at 441 cm^{-1} further confirmed indicate a successful fluoride adsorption. [40]. Based on the results above, we can conclude that the adsorbent CS-ZFA can successfully adsorb F^-.

The distribution of elements in the CS-ZFA-F composite was observed by ??were. As shown in Figure 4, Fe, Al, Zr and F were were uniformly dispersed on the adsorbent. This indicates that the metal elements well reacted with chitosan matrix and the F^- were well adsorbed onto the active sites.

TG analysis was conducted to understand the thermal stability of CS and CS-ZFA. It can be seen from Figure 5 that chitosan (CS) began to lose weight when the temperature rises to 100 ℃ , which was mainly due to the loss of free water and bound water in the chitosan microspheres. With the further increase of temperature to 530 ℃, CS lost 30% of its weight. and the mass tended to be stable, which was mainly due to the fact that chitosan gradually carbonized and decomposed during this process. The weight loss of CS-ZFA in the range of 30~800 ℃ was mainly divided into two stages. In the first stage, the mass loss of CS-ZFA was 22.1% at 30~204 ℃, which was attributed to the volatilization of free water and part of bound water in the

microsphere. In the second stage, the weight loss rate within 204-554 ℃ was higher than that in 30~204 ℃, but much lower than that of CS. This might be due to the introduction of metal ions in CS-ZFA as metal ions can coordinate with hydroxyl and amino groups, making it difficult to lose the combined water. The weight loss rate of CS-ZFA at temperature above 554℃ was similar to that of CS. when the sample weight loss reached about 40% and the mass tended to be stable, leaving some zirconium, iron and aluminum oxides. In general, the weight loss rate of CS-ZFA was lower than that of CS, and the final residual mass percentage of CS-ZFA was about 10% higher than that of CS due to introduced inorganic metals. Therefore, the thermal stability of the chitosan microspheres has been improved due to the successful addition of the metals Zr/Al/Fe.

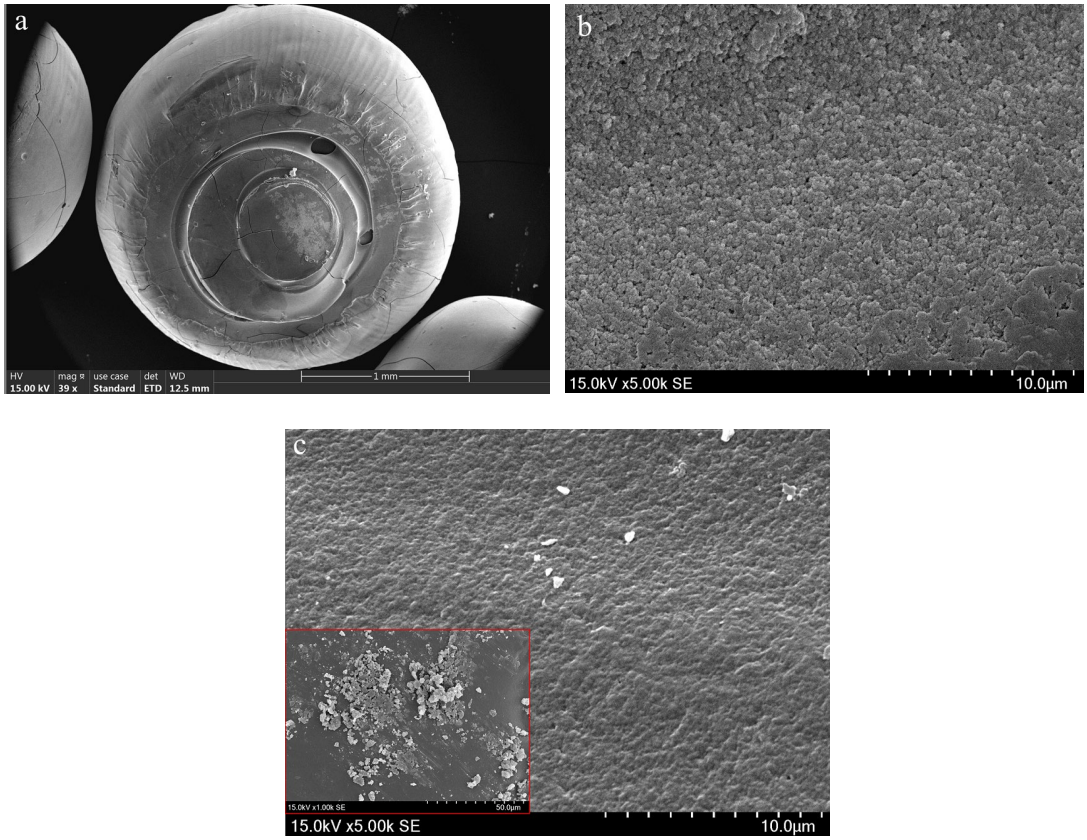

Fig. 1 SEM pattern of CS-ZFA sample (a, b): SEM image of CS-ZFA before adsorption; (c) SEM image of CS-ZFA after adsorption

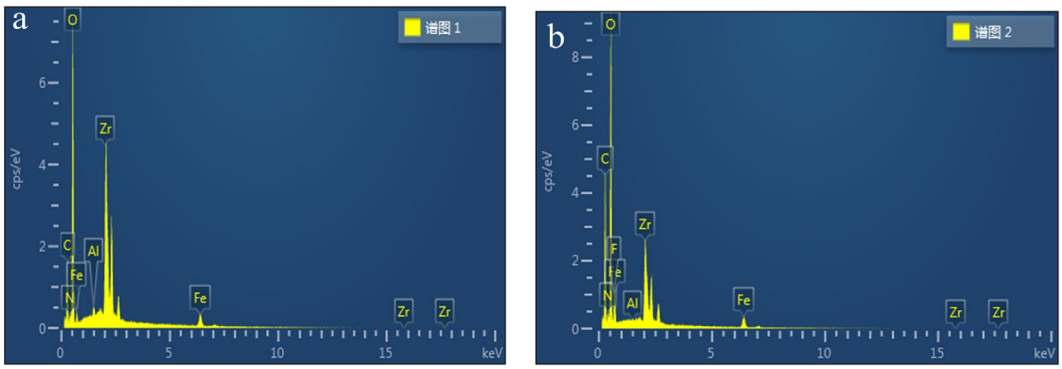

Fig. 2 EDS pattern of CS-ZFA sample (a) CS-ZFA before adsorption; (b) CS-ZFA after adsorption

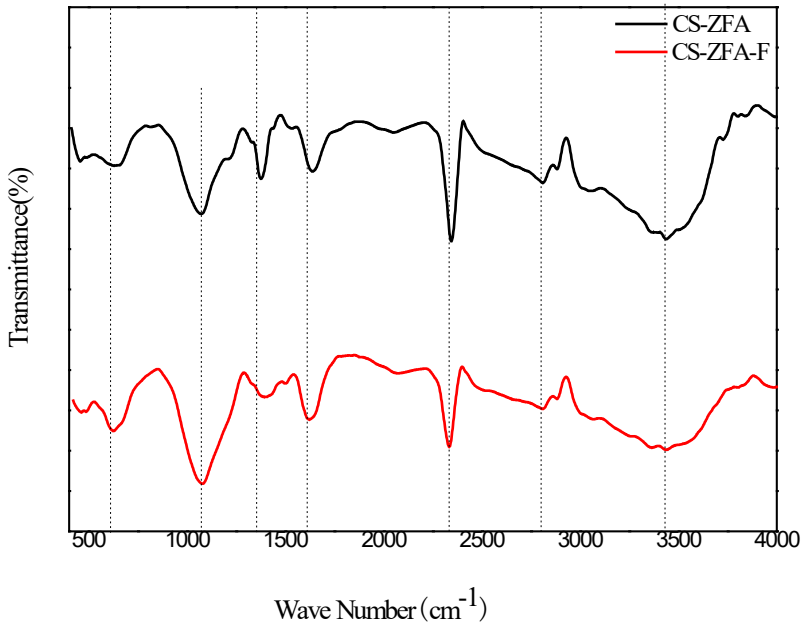

Fig. 3 FTIR spectra of CS-ZFA before and after adsorption

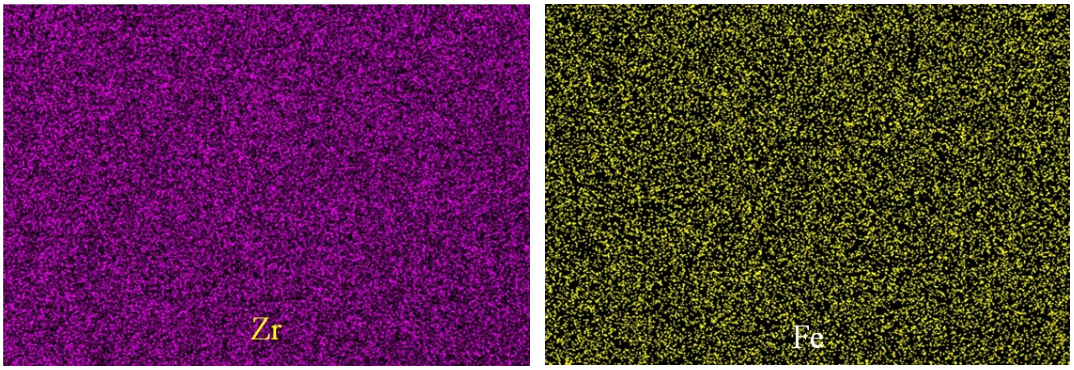

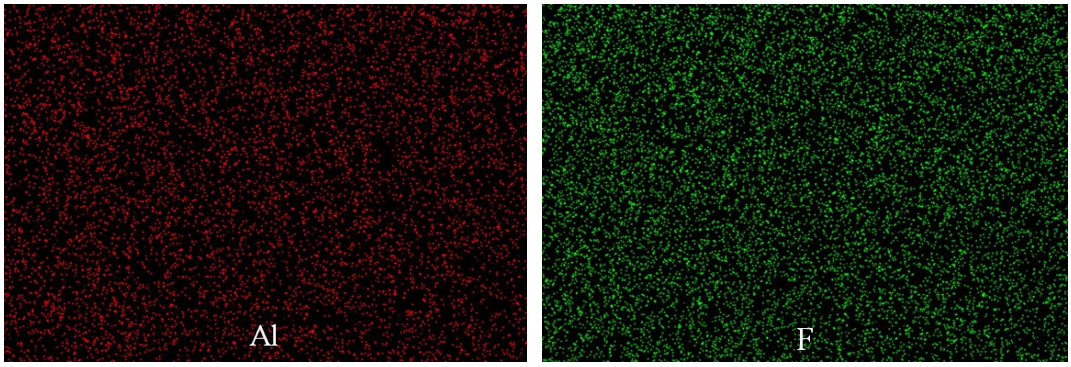

Fig. 4 Elemental mapping of CS-ZFA after adsorption of fluoride

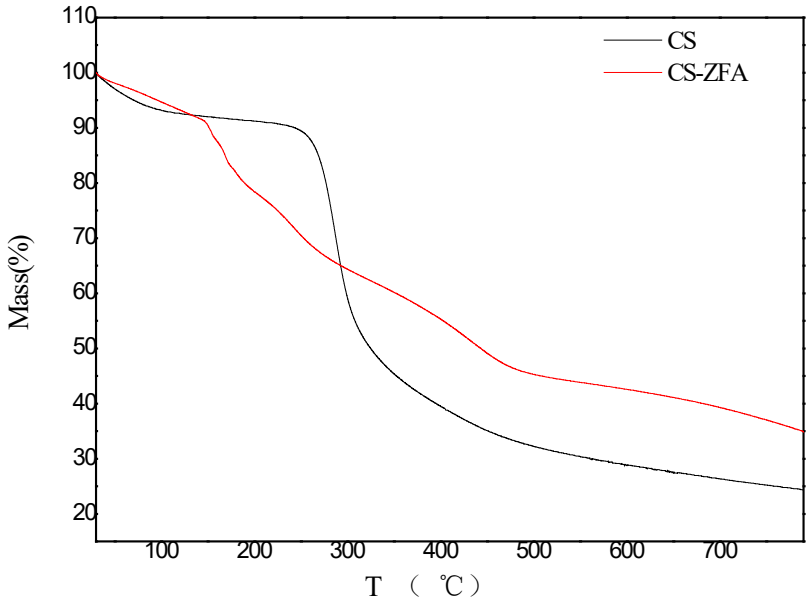

Fig. 5 TG curves of CS and CS-ZFA

3.2 evaluation of fluoride adsorption by using absorbent CS-ZFA

Different doses of CS and CS-ZFA for fluoride adsorption were investigated with an initial fluoride concentration of 60 mg/L at pH of 6.0. It can be seen from Figure 6 that the maximum fluoride adsorption capacity is 11.91 mg/g by CS while it reached 36.04 mg/g by using CS-ZFA, two times higher than CS. . This comparison experiment demonstrates that chitosan modified by Fe/Al/Zr can increase its fluoride adsorption capacity significantly.

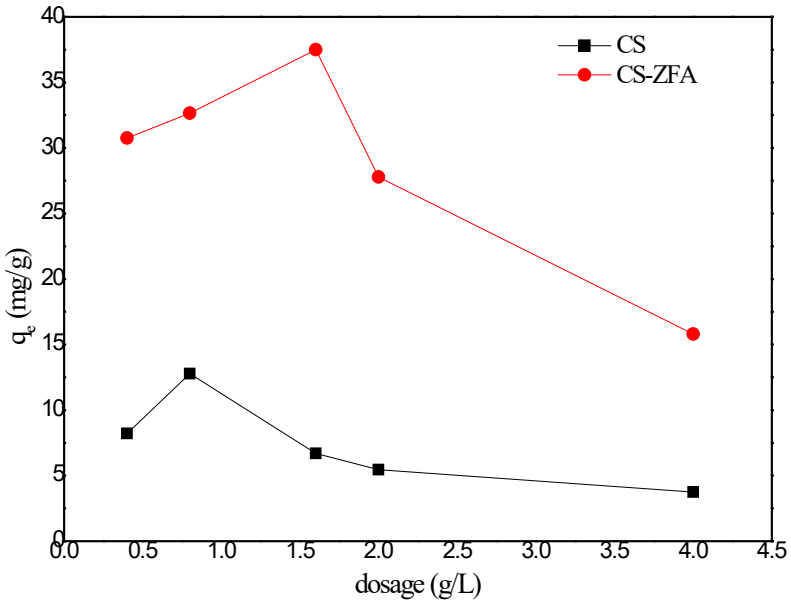

Fig. 6 The fluoride adsorption by CS and CS-ZFA with different dosages (m_{CS-ZFA}=1.6 g/L; C_0=60 mg/L; t=120 min)

3.2 Effects of pH on adsorption by CS-ZFA

The properties of adsorbent and adsorbate change with the solution pH, so it is necessary to investigate the effects of pH on the fluoride adsorption by CS-ZFA [41]. It can be seen from Figure 7 that the adsorption capacity of CS-ZFA was only 27.67mg/g in a pH range of 2.0-4.0 and , and it increased to 35.72 mg/g at pH of 5.0. When pH was further increased from 5.0 to 7.0, there was no significant difference in adsorption capacity. When pH continue to increase to alkaline range, the adsorption capacity dropped significantly. From this pH study, it can be known that CS-ZFA had a relatively wide range of pH, i.e.,5.0 - 7.0, for optimal fluoride adsorption. At lower pHs, the hydrolysis reaction of Fe^{3+}, Al^{3+} and Zr^{4+} produced a large amount of H^+, which enhanced the protonation ofamino groups on the surface of the chitosan microspheres. The positively charged adsorbent surface has higher potential to attract

the negatively charged fluoride via electrostatic interaction [42, 43]. In the pH range of 5.0~7.0, there was also the coordination reaction between metal ions (Fe^{3+}, Al^{3+}, Zr^{4+}) chelated with chitosan and F^-,. increasing the adsorption capacity of CS-ZFA to F^-. In alkaline condition, a large amount of OH^- compete with F^- for the active sites on CS-ZFA [44], and there was no protonated amino groups. These two factors led to a reduced adsorption capacity. Therefore, pH 6.0 was selected for the subsequent adsorption experiments.

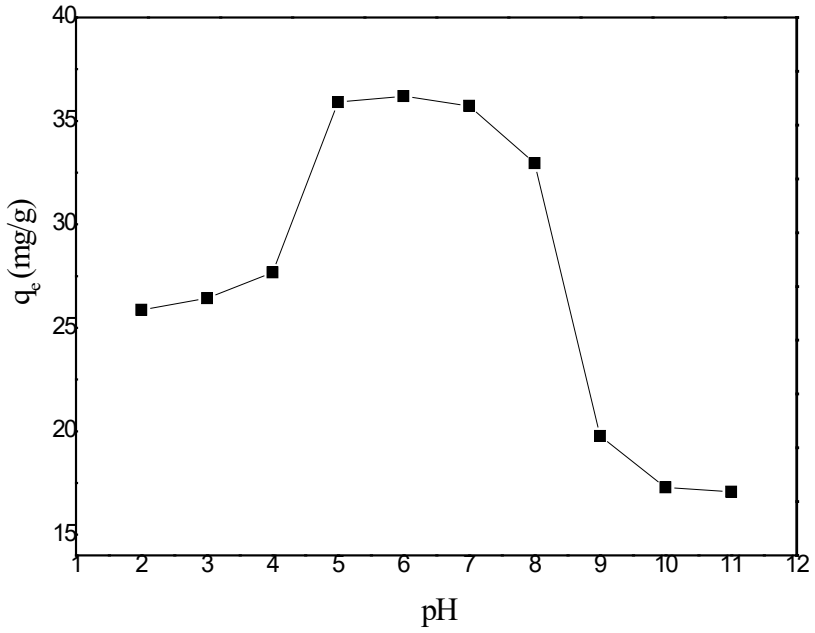

Fig. 7 Effects of pH on fluoride adsorption by CS-ZFA ($m_{CS\text{-}ZFA}$=1.6 g/L; C_0=60 mg/L; t=120 min)

3.3. Effects of initial fluoride concentration and adsorbent dosage on adsorption capacity

The optimal adsorption capacity of CS-ZFA to F^- was studied under different fluoride concentrations and adsorbent dosages. The adsorption time was set at120 min, and reaction solution pH was set at 6.0. It can be seen from Figure 8 that the

adsorption capacity of CS-ZFA to F^- increased with the initial concentrations of fluoride with all dosages studied. When the initial concentration of F^- was fixed at a value, the highest adsorption capacity, i.e., 35.91 mg/g, was found with an absorbent dosage of 1.6 g/L. Because there were more coordination sites on $-NH_2$ and the three metal ions available for F^- adsorption, the adsorption did not reached saturation, which resulted in a low adsorption capacity at lower initial fluoride concentration[45]. Once the adsorption reaches saturation, the adsorption capacity cannot increase anymore. The number of effective adsorption sites was not linearly related to the amount of adsorbent. As the adsorbent dosage increases, the active sites on the adsorbent increase correspondingly to adsorb more fluoride until adsorption saturation. [46].

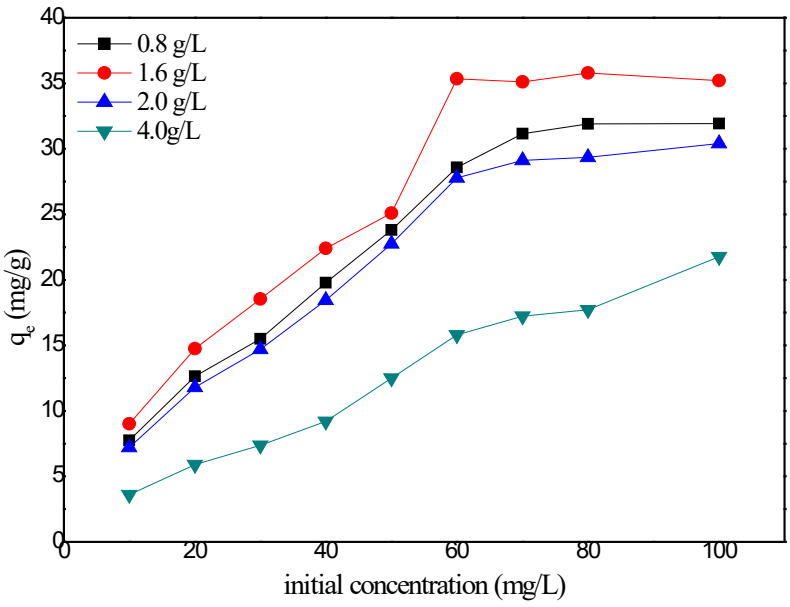

Fig. 8 Effects of initial concentrations of fluorine and dosage of CS-ZFA on the adsorption capacity of CS-ZFA (pH=6.0; t=120min)

3.4 Effect of adsorption time

Adsorption time is an important parameter to determine the adsorption efficiency. Thus, fluoride adsorption by CS-ZFA with adsorption duration of 10~360 min was investigated. As shown in Figure 9, the removal rate of F^- increased with the extension of adsorption time. In the first 50 minutes, the adsorption capacity the removal rate of F^- reached 33.14 mg/g, and 79.47%, respectively. In the subsequent 40 minutes, there was no obvious change regarding the adsorption capacity although a very slight increase was still observed, resulting in a final adsorption capacity of 34.57 mg/g and the maximum fluoride removal rate - of 82.90% after 360-min adsorption. Thus, it is believed that a saturation can be reached within 50 minutes in the conditions studied. But for insurance, 120 min was selected as an adsorption duration for the subsequent experiments.

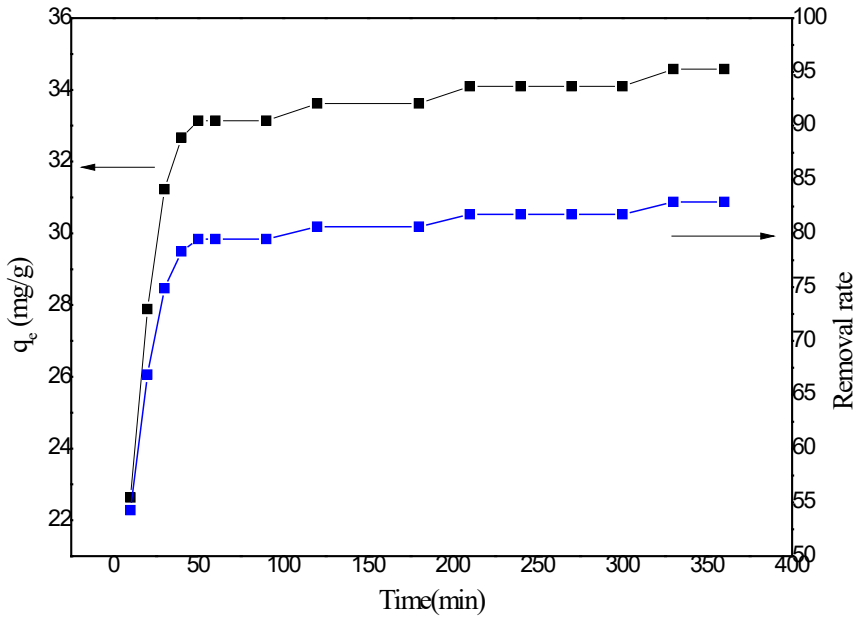

Fig. 9 Effect of adsorption time on the adsorption capacity and fluoride removal rate by CS-ZFA (pH=6.0; $m_{CS\text{-}ZFA}$=1.6 g/L; C_0=60 mg/L)

3.5 Effect of coexisting ions

Wastewater usually contains other types of anions, which could compete with fluoride to reduce the fluoride removal rate by adsorbents. Thus, a higher selectivity of absorbent is better regarding operation cost. of The commonly present anions together with F-1 in wastewater are Cl^-, SO_4^{2-}, NO_3^- and PO_4^{3-} , which were was studied in two different concentrations such as 1 and 10mM to understand their competition with fluoride. From Figure 10, it can be seen that the fluoride adsorption was almost not affected by the presence of Cl^- or NO_3^- range with concentrations of 1 or 10mM (Figure 10). However, the presence of SO_4^{2-} and PO_4^{3-} show an obvious interference on the fluoride adsorption [47]. When the concentration of SO_4^{2-} was 10mM, the adsorption of fluoride reduced by about 44%. when the concentration of PO_4^{3-} was 1mM, the adsorption capacity decreased by 50.40%. These results show that the metal ions on CS-ZFA surface had a stronger affinity to F^- than to monovalent ions such as Cl^- and NO_3^-. Divalent and trivalent such as SO_4^{2-} and PO_4^{3-} have more negative electrons to combine with the positive charges of metal ions on the adsorbent, resulting in reduced adsorption capacity of F^-.

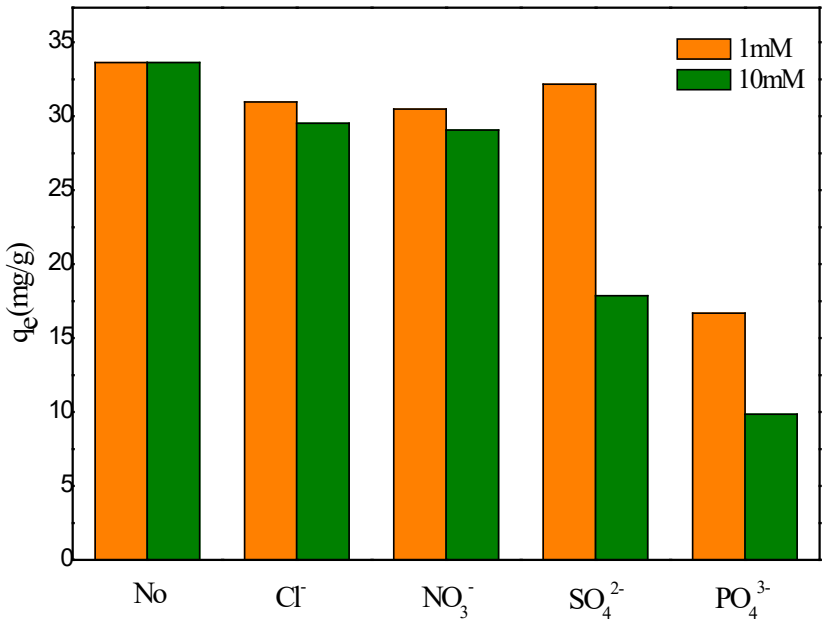

Fig. 10 Effect of the coexisting anions on the adsorption of fluoride by CS-ZFA (pH=6.0; $m_{CS\text{-}ZFA}$=1.6 g/L; C_0=60 mg/L; t=120min)

3.7 The adsorption isotherm

Langmuir and Freundlich isotherm models were used to simulate the experimental data to explore the relationship between the adsorbent and adsorbate, which can shed insight on adsorption mechanism. At room temperature (298.2K), the adsorption isotherm of fluoride by CS-ZFA absorbent was shown in Figure 11.

The Langmuir isotherm model was based on assumption of a monolayer adsorption on the adsorbent surface, while the Freundlich isotherm model assumes a heterogeneous surface and a multilayer adsorption with an energetic non-uniform distribution [15, 20]. Langmuir isotherm model can be expressed as follows:

$$\frac{C_e}{q_e} = \frac{C_e}{q_{\max}} + \frac{1}{q_{\max} K_L} \qquad (2)$$

Where, q_e and C_e were equilibrium adsorption capacity (mg/g) and equilibrium

concentration (mg/L), q_{max} was the maximum adsorption capacity (mg/g), and K_L was the Langmuir constant (L/mg).

Freundlich model can be expressed as follows:

$$\log q_e = \log K_f + \frac{1}{n}\log C_e \qquad (3)$$

Where, q_e and C_e were the equilibrium concentration (mg/L) and equilibrium adsorption capacity (mg/g), K_f and n were the Freundlich constants.

The experimental data was performed regression analysis with multi-dimensional linear regression analysis, then regression coefficient (R^2) was obtained and experimental curve was fitted. the parameters of Langmuir model and Freundlich isothermal model were calculated with ?? what? Method? which were presented in Table 1. the maximum adsorption capacity calculated from the Langmuir model was 36.04 mg/g, which was close to the experimental valueThe correlation coefficients (R^2) for both Langmuir and Freundlich isotherm models are above 0.96, indicating that both models fit well with the fluoride adsorption by CS-ZFA. This might suggest that the fluoride might be adsorbed on the surface of adsorbent in the mixed forms of monolayer and multilayer.

Table 2 shows the comparison of adsorption capacity of different adsorbents. It can be seen that the adsorption capacity of fluoride by CS-ZFA developed in this study is similar to that La/ Li/Al Layered Double Hydroxides, but much higher than other types of adsorbents. Given the easy availability of CS and low cost of CS-ZFA compared with La/ Li/Al Layered Double Hydroxides, the newly developed CS-ZFA is a promising adsorbent to deal with wastewater with excessive fluorine content.

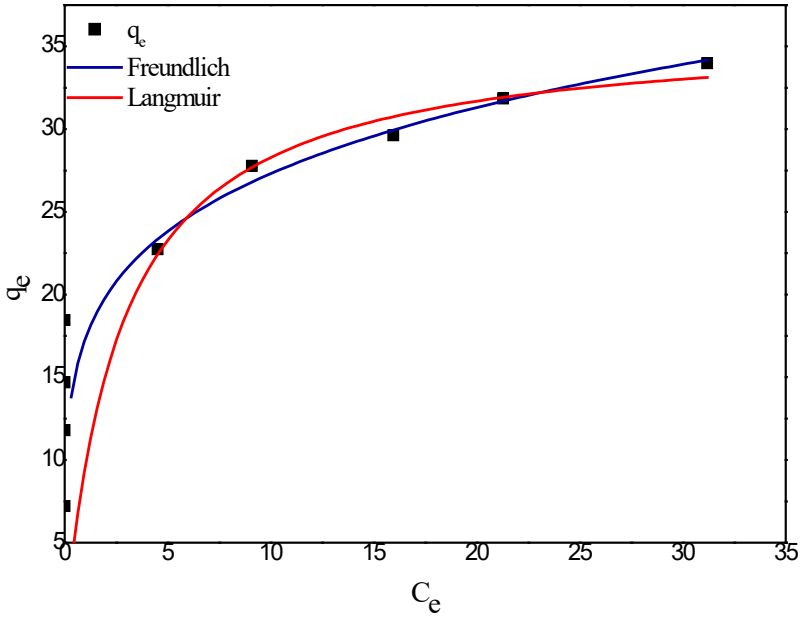

Fig. 11 Simulated adsorption with Langmuir isotherm model and Freudlich isotherm model

Table 1 Langmuir and Freundlich isothermal model parameters for the adsorption of fluoride by CS-ZFA

	Langmuir isothermal model			Freundlich isothermal model		
Fluoride	b(L/mg)	q_{max} (mg/g)	R^2	K_f (mg/g)	n	R^2
F^-	0.3651	36.0360	0.9617	17.3435	5.0715	0.9728

Table 2 Comparison of fluoride removal capacities by different adsorbents

Adsorbent	Adsorption capacity (mg/g)	Reference
La/ Li/Al Layered Double Hydroxides	35.40	[48]
Fe-Al-Ce composite	2.22	[49]

Hydrous Zirconium Oxide-Impregnated Chitosan Beads	22.16	[50]
Oxalic acid mediated polyacrylamide-Zr complex	9.64	[51]
Mg-Al-Zr composite	22.91	[3]
alumina/chitosan composite	23.18	[22]
CS-ZFA	36.06	This study

3.4 The adsorption kinetics of CS-ZFA

To understand the potential rate-limiting step in the fluoride adsorption by CS-ZFA, the pseudo-first-order, the pseudo-second-order and intra-particle diffusion kinetics models, expressed respectively as below [48, 49], were applied to evaluate the adsorption kinetic parameters.

$$\ln(q_e - q_t) = \ln q_e - k_1 t \quad (4)$$

$$\frac{t}{q_t} = \frac{1}{k_2 q_e^2} + \frac{t}{q_e} \quad (5)$$

$$q_t = k_p t^{\frac{1}{2}} + C \quad (6)$$

Where, q_e (mg/g) is the amount of adsorbed fluoride at equilibrium by per gram CS-ZFA, and q_t (mg/g) is the amount of adsorbed fluoride at time t; k_1 (1/min), k_2 (g/(mg min)) and k_p (mg/(g $min^{1/2}$)) are the rate constants of the pseudo-first-order, pseudo-first-order model and intra-particle diffusion model, respectively, C (mg/g) is the constant of intra-particle diffusion model, which is proportional to the thickness of the boundary layer.

The fitted lines by the three different kinetic models are shown in Figure 12 and the corresponding parameters are listed in Table 3. As we can see, the correlation coefficient (R^2=0.9503) of the pseudo-second-order model is slightly higher than pseudo-first-order model (R^2=0.9477), and the calculated equilibrium adsorption capacity q_e, i.e., 35.1124 mg/g, is closer to the experimental value (35.9134 mg/g). This indicated that the adsorption process is more controlled by chemisorption. On the other hand, it can be seen from Figure 12b that the fitting of experimental data by using intra-particle diffusion kinetic model produced two distinctive linear curves during two adsorption stages. This might suggest that the adsorption during two adsorption stages is controlled by different adsorption mechanisms. The first straight linear portion present the film diffusion, which may be the external surface adsorption, and the intra-particle diffusion step, the second stage presented the final equilibrium adsorption [50]. The constants *C* was not zero and the liner line did not pass the origin, demonstrating that intra-particle diffusion was not the rate controlling step [51]. (When you used kinetic models to explain the adsorption rate controlling steps and etc. pls explain the kinetics themselves first, especially the meaning of each kinetic parameter)

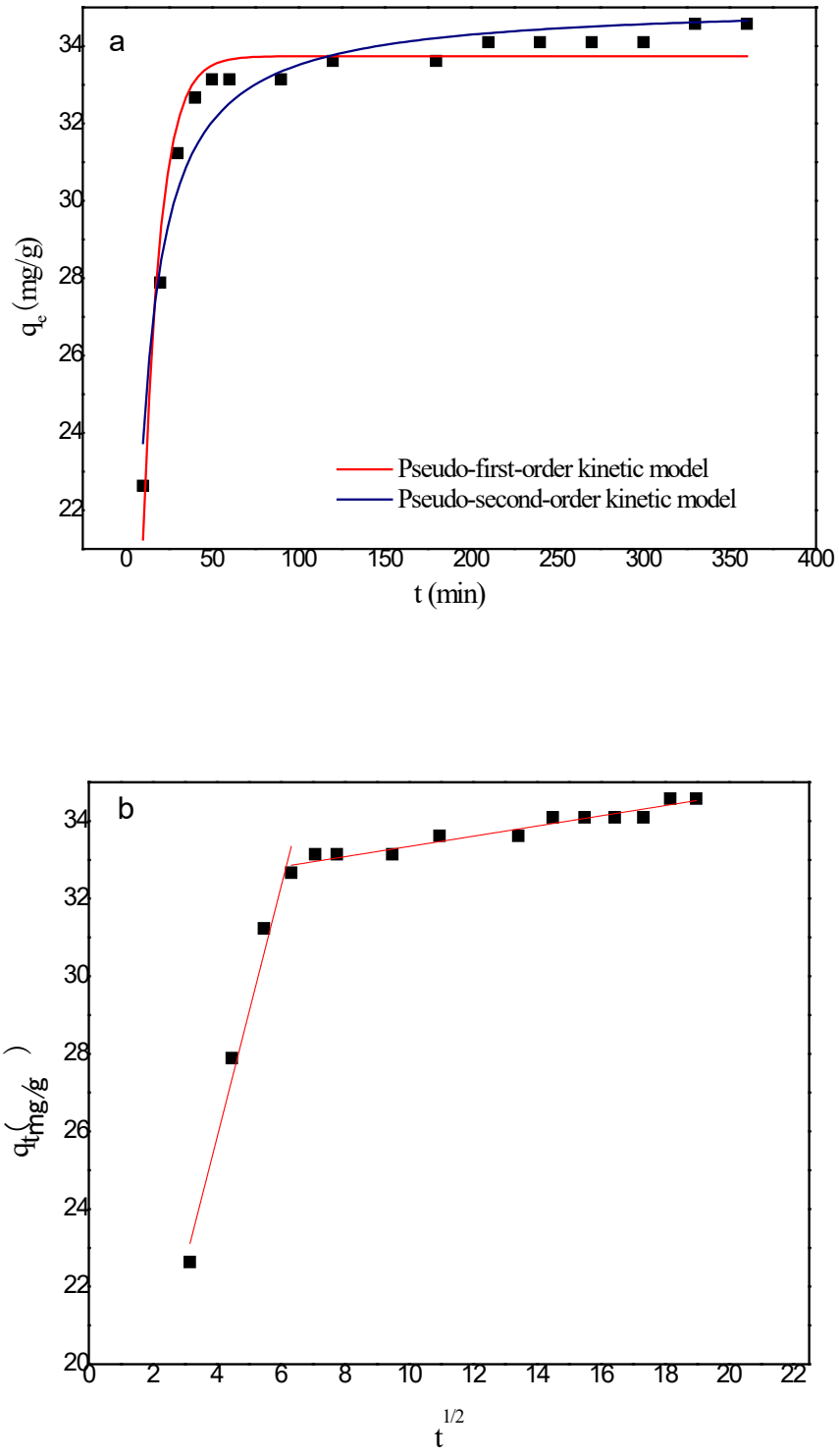

Fig. 12 Pseudo-first-order and pseudo-second-order models for fluoride adsorption (a); the plot of intra-particle diffusion model for fluoride adsorption (b) (pH=6, $m_{CS\text{-}ZFA}$=1.6 g/L, C_0=60 mg/L)

Table 3 Calculated kinetic parameters for the adsorption of fluoride onto CS-ZFA composite (adsorbent dose: 1.6 g/L, fluoride concentration: 60 mg/L and pH: 6.0).

Pseudo-first-order		K_1	q_e	R^2
model		0.0994	33.7399	0.9477
Pseudo-second-order		K_2	q_e	R^2
model		0.0059	35.1124	0.9503
		k_p	C	R^2
Intra-particle	Step I	3.2344	12.8876	0.9654
diffusion parameters	Step II	0.1316	32.0277	0.9316

3.7. Regeneration of CS-ZFA for reuse

To use the adsorbent developed in this study repeatedly and further reduce the cost, it is very essential to investigate the regeneration ability of the adsorbent. In the present study, 0.1M HCl and 0.1M NaCl, respectively, was used to regenerate CS-ZFA [52]. It was observed in Figure 13 that the adsorbent had a good regeneration performance. According to the figure, the composite can be used after three regeneration cycles. These results indicated that the composite had the good potential for fluoride removal in the practical application.

Supplement why HCl and NaOH can regenerate CS-ZFA. What is the principle?

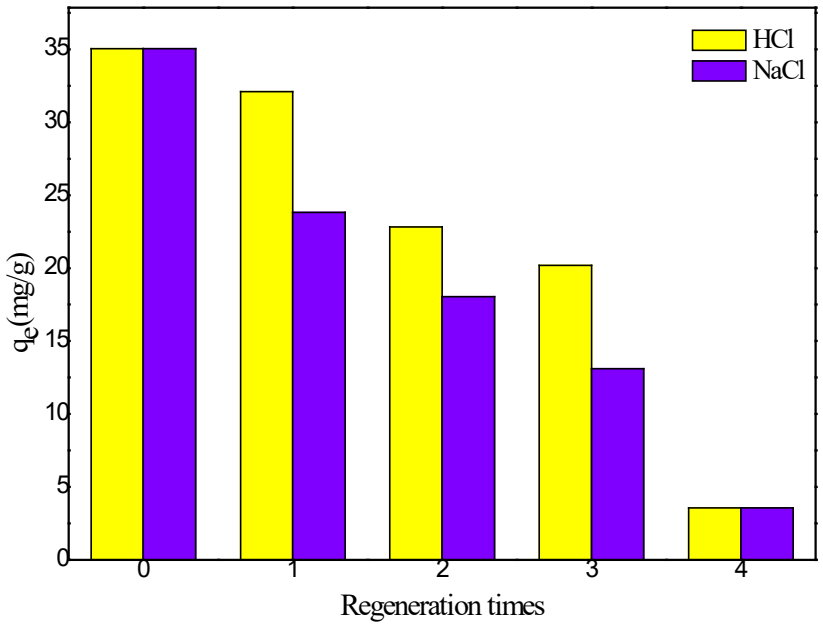

Fig. 13 Regeneration study on the F^- removal by CS-ZFA

4. Conclusions

chitosan modified by zirconium, aluminum and iron, named as CS-ZFA, was successfully developed as an novel adsorbent to remove fluoride from contaminated water with a maximum adsorption capacity of ?? in the studied conditions. The results indicate that the addition of zirconium, aluminum and iron to the chitosan matrixenable the active amino groups and hydroxyl groups in the raw chitosan to chelate with added metal ions to form new stable complexes. The chelated metal ions become the new adsorption sites to increase the fluoride adsorption by CS-ZFA [53]. the introduction of Fe/Al/Zr significantly enabled its excellent adsorption performance over a wide pH range. More preferably, the adsorbent can be used directly in the general discharge water without adjusting the pH. The fluoride

adsorption by CS-ZFA was in good compliance with the pseudo-second-order kinetics and intra-particle diffusion model, indicating that the adsorption rate was mostly determined by chemical adsorption, and there were also pore adsorption and ion exchange. The fluoride adsorption by CS-ZFA can be explained by either Langmuir or Freundlich models, indicating that the adsorption of CS-ZFA on F^- was a relatively complex adsorption process. For monovalent ions, CS-ZFA has higher selectivity on fluoride than Cl^- and NO_3^- , but divalent and trivalent ions such as ?? and ?? interfered fluoride adsorption . At the same time, the composite could be reused for three times without much loss of adsorption capacity which has greatly improved the values of the adsorbent.

Acknowledgements

References:

[1] Hernández-Campos, M., et al., Lanthanum-doped silica xerogels for the removal of fluorides from waters. Journal of Environmental Management, 2018, 213: 549-554.

[2] Lin, K. Y. A., Y. T. Liu and S. Y. Chen, Adsorption of fluoride to UiO-66-NH_2 in water: Stability, kinetic, isotherm and thermodynamic studies. Journal of Colloid & Interface Science, 2016, 461: 79-87.

[3] Wang, M., et al., Removal of fluoride from aqueous solution by Mg-Al-Zr Triple-metal composite. Chemical Engineering Journal, 2017, 322: 246-253.

[4] Zhu, T., et al., Enhanced adsorption of fluoride by cerium immobilized cross-linked chitosan composite. Journal of Fluorine Chemistry, 2017, 194: 80-88.

[5] Reardon, E. J., A Limestone Reactor for Fluoride Removal from Wastewaters. Environmental Science & Technology, 2000, 34(15): 3247-3253.

[6] Turner, B. D., B. Philip and S. L. S. Stipp, Fluoride removal by calcite: evidence for fluorite precipitation and surface adsorption. Environmental Science & Technology, 2005, 39(24): 9561-9568.

[7] Kaisa,V., et al., Removal of metals and anions from drinking water by ion exchange. Desalination, 2003, 155(2): 157-170.

[8] Viswanathan, N. and S. Meenakshi, Role of metal ion incorporation in ion exchange resin on the selectivity of fluoride. Journal of Hazardous Materials, 2009, 162(2-3): 920-930.
[9] Richards, L. A., M. Vuachère and A. I. Schäfer, Impact of pH on the removal of fluoride, nitrate and boron by nanofiltration/reverse osmosis. Desalination, 2010, 261(3): 331-337.
[10] Farjami, M., A. Moghadassi and V. Vatanpour, Modeling and simulation of CO_2 removal in a polyvinylidene fluoride hollow fiber membrane contactor with computational fluid dynamics. Chemical Engineering & Processing Process Intensification, 2015, 98: 41-51.
[11] Hichour, M., et al., Fluoride removal from waters by Donnan dialysis. Separation & Purification Technology, 1999, 18(1): 1-11.
[12] Ruiz, T., et al., Modelisation of fluoride removal in Donnan dialysis. Journal of Membrane Science, 2003, 212(1): 113-121.
[13] Yu, Y., L. Yu and J. Paul Chen, Adsorption of fluoride by Fe-Mg-La Triple-metal composite: Adsorbent preparation, illustration of performance and study of mechanisms. Chemical Engineering Journal, 2015, 262: 839-846.
[14] Zhou, J., et al., Highly selective and efficient removal of fluoride from ground water by layered Al-Zr-La Tri-metal hydroxide. Applied Surface Science, 2018, 435: 920-927.
[15] Chi, Y., et al., Preparation of Mg-Al-Ce Triple-metal composites for fluoride removal from aqueous solutions. Journal of Molecular Liquids, 2017, 242: 416-422.
[16] Zhao, X., et al., The stability and defluoridation performance of MOFs in fluoride solutions. Microporous and Mesoporous Materials, 2014, 185: 72-78.
[17] Mohapatra, D., et al., Use of oxide minerals to abate fluoride from water. Journal of Colloid & Interface Science, 2004, 275(2): 355-359.
[18] Sepehr, M. N., et al., Defluoridation of water via Light Weight Expanded Clay Aggregate (LECA): Adsorbent characterization, competing ions, chemical regeneration, equilibrium and kinetic modeling. Journal of the Taiwan Institute of Chemical Engineers, 2014, 45(4): 1821-1834.
[19] Lv, L., Defluoridation of drinking water by calcined MgAl-CO_3 layered double hydroxides. Desalination, 2007, 208(1): 125-133.
[20] Liu, H., et al., Preparation of Al-Ce hybrid adsorbent and its application for defluoridation of drinking water. Journal of Hazardous Materials, 2010, 179(1): 424-430.
[21] Sujana, M. G., A. Mishra and B. C. Acharya, Hydrous ferric oxide doped alginate beads for fluoride removal: Adsorption kinetics and equilibrium studies. Applied Surface Science, 2013, 270(14): 767-776.
[22] Viswanathan, N. and S. Meenakshi, Enriched fluoride sorption using alumina/chitosan composite. Journal of Hazardous Materials, 2010, 178(1): 226-232.
[23] Swain, S. K., T. Patnaik and R. K. Dey, Efficient removal of fluoride using new composite material of biopolymer alginate entrapped mixed metal oxide nanomaterials. Desalination and Water Treatment, 2013, 51(22-24): 4368-4378.
[24] Wang, H., et al., Defluoridation of drinking water by Mg/Al hydrotalcite-like compounds and their calcined products. Applied Clay Science, 2007, 35(1): 59-66.
[25] Moriyama, S., K. Sasaki and T. Hirajima, Effect of calcination temperature on Mg-Al bimetallic oxides as sorbents for the removal of F- in aqueous solutions. Chemosphere, 2014. 95(1): 597-603.
[26] Nasr, A. B., et al., Fluoride removal from aqueous solution by Purolite A520E resin: kinetic and thermodynamics study. Desalination & Water Treatment, 2015, 54(6): 1604-1611.
[27] Li, K., et al., Efficient adsorption of both methyl orange and chromium from their aqueous

mixtures using a quaternary ammonium salt modified chitosan magnetic composite adsorbent. Chemosphere, 2016, 154: 310-318.
[28] Anush, S. M., et al., Heterocyclic modification of chitosan for the adsorption of Cu (II) and Cr (VI) ions. Separation Science and Technology, 2018, 53(13): 1979-1990.
[29] Chethan, P. D. and B. Vishalakshi, Synthesis of ethylenediamine modified chitosan microspheres for removal of divalent and hexavalent ions. International Journal of Biological Macromolecules, 2015, 75: 179-185.
[30] Guibal, E., E. Touraud and J. Roussy, Chitosan Interactions with Metal Ions and Dyes: Dissolved-state vs. Solid-state Application. World Journal of Microbiology & Biotechnology, 2005, 21(6-7): 913-920.
[31] Wang M., Yu X., Yang C., et al. Removal of fluoride from aqueous solution by Mg-Al-Zr Triple-metal composite. Chemical Engineering Journal, 2017, 322(12): 246-253.
[32] Yu Y., Yu L., Paul Chen J. Adsorption of fluoride by Fe-Mg-La Triple-metal composite: Adsorbent preparation, illustration of performance and study of mechanisms. Chemical Engineering Journal, 2015, 262(36): 839-846.
[33] Zhiqian Jia, Shuang Hao, Xiaoyu Lu. Exfoliated Mg-Al-Fe layered double hydroxides/polyether sulfone mixed matrix membranes for adsorption of phosphate and fluoride from aqueous solutions. Journal of Environmental Sciences, 2018, 8: 63-73.
[34] Marwa M. Sobeih, et al. Glauconite clay-functionalized chitosan nanocomposites for efficient adsorptive removal of fluoride ions from polluted aqueous solutions. RSC Advances, 2020, 10(43): 25567-25585.
[35] Zhu T., Huang W., Zhang L., et al. Adsorption of Cr(VI) on cerium immobilized cross-linked chitosan composite in single system and coexisted with Orange II in binary system. International Journal of Biological Macromolecules, 2017, 103(14): 605-612.
[36] Cho D W, Jeon B H, Jeong Y, et al. Synthesis of hydrous zirconium oxide-impregnated chitosan beads and their application for removal of fluoride and lead. Applied Surface Science, 2016, 372(MAY.30): 13-19.
[37] Zhang, M., et al. Novel cationic polymer modified magnetic chitosan beads for efficient adsorption of heavy metals and dyes over a wide pH range. International Journal of Biological Macromolecules, 2020, 156: 289-301.
[38] Qian J., Lin X., Zhou Q. Study on adsorption properties of modified magnetic chitosan microspheres for fluoride .New Chemical Materials, 2016, 44(11): 146-149.
[39] Li L., Zhu Q., Man K., et al. Fluoride removal from liquid phase by Fe-Al-La trimetal hydroxides adsorbent prepared by iron and aluminum leaching from red mud. Journal of Molecular Liquids, 2017, 237(45): 164-172.
[40] Liu Q. Study on the adsorption characteristics of fluoride in water by rare metal modified chitosan derivatives. Northwest A&F University, 2016.
[41] Tripathy, S., et al., Removal of fluoride from drinking water by adsorption onto alum-impregnated activated alumina. Separation & Purification Technology, 2006, 50(3): 310-317.
[42] Dongjuan, et al., Novel Al-doped carbon nanotubes with adsorption and coagulation promotion for organic pollutant removal. Journal of Environmental Sciences, 2016, 54(4): 1-12.
[43] Li, L., et al., Fluoride removal from liquid phase by Fe-Al-La trimetal hydroxides adsorbent prepared by iron and aluminum leaching from red mud. Journal of Molecular Liquids, 2017, 237: 164-172.

[44] Sowmya A., Meenakshi S. An efficient and re-generable quaternary amine modified chitosan beads for the removal of nitrate and phosphate anions. Journal of Environmental Chemical Engineering, 2013, 1(4): 906-915.
[45] Hu Q., Chen N., Feng C., et al. Nitrate adsorption from aqueous solution using granular chitosan-Fe^{3+} complex. Applied Surface Science, 2015, 347: 1-9.
[46] Wang M., Yu X., Yang C., et al. Removal of fluoride from aqueous solution by Mg-Al-Zr triple-metal composite. Chemical Engineering Journal, 2017, 322(1): 246-253.
[47] Yang Y., Ling Y., J. Paul Chen. Adsorption of fluoride by Fe-Mg-La triple-metal composite: Adsorbent preparation, illustration of performance and study of mechanisms. Chemical Engineering Journal, 2015, 15(262): 839-846.
[48] Zhao, X., et al., Enhanced fluoride removal by La-doped Li/Al layered double hydroxides. Journal of Colloid & Interface Science, 2018, 509: 353-359.
[49] Chen, L., et al., Granulation of Fe-Al-Ce nano-adsorbent for fluoride removal from drinking water by spray coating on sand in a fluidized bed. Powder Technology, 2009, 193(1): 59-64.
[50] Cho, D. W., et al., Synthesis of hydrous zirconium oxide-impregnated chitosan beads and their application for removal of fluoride and lead. Applied Surface Science, 2016, 372: 13-19.
[51] Yan, J., et al., Adsorption of heavy metals and methylene blue from aqueous solution with citric acid modified peach stone. Separation Science and Technology, 2018, 53(11): 1678-1688.
[52] Zhang M., Zhang Z., et al., Novel cationic polymer modified magnetic chitosan beads for efficient adsorption of heavy metals and dyes over a wide pH range. International Journal of Biological Macromolecules, 2020, 156: 289-301.
[53] Khan, H. and S. Sharma, Next-generation organometallic adsorbents for safe removal of excessive fluoride from aqueous systems. Journal of Applied Polymer Science, 2019, 136(4): 46993.